Supporting Information

Ten Nanometer Scale WO_3/CuO Heterojunction Nanochannel for an Ultrasensitive Chemical Sensor

Soo-Yeon Cho[†,‡,⊥], *Doohyung Jang*[†,‡,⊥], *Hohyung Kang*[†,‡], *Hyeong-Jun Koh*[†,‡], *Junghoon Choi*[†,‡], *and Hee-Tae Jung*[*,†,‡]

[†] Department of Chemical and Biomolecular Engineering (BK-21 Plus), Korea Advanced Institute of Science and Technology (KAIST), Daejeon 34141, Republic of Korea

[‡] KAIST Institute for NanoCentury, Yuseong-gu, Daejeon 34141, Republic of Korea

[⊥] These authors contributed equally to this work

Table of contents:

Experimental Section

Fabrication of the p–n heterojunction nanochannel: A thin PS film (M_w = 18,000 g mol^{-1}, 5 wt% solution in anhydrous toluene) was spin-coated onto a Si wafer substrate with a 200 nm thick layer of deposited SiO_2. A PDMS mold (Sylgard 184, 10:1 (w/w) prepolymer/curing agent; Dow Corning) was pressed onto the PS spin-coated surface, which was then heated above the glass transition temperature (135°C) in a vacuum oven to introduce PS into the mold voids by capillary force. The PDMS mold was then replicated from a silicon master consisting of a line pattern with a depth of 400 nm and spacing and width of 500 nm. After the polymer prepattern was formed, the residual polymer at the bottom of the prepattern was removed by RIE using a mixture of O_2 (40 sccm) and CF_4 (60 sccm) plasma at a chamber pressure of 20 mTorr and a power density of 80 W. After residual removal, a 30 nm thick film of n-type and p-type metals (W and Cu) was sequentially deposited (e.g., Cu: 0.3 nm/W: 29.4 nm/Cu: 0.3 nm) on the prepattern by e-beam evaporation. The prepatterned surface was ion milled with Ar^+ gas by dc sputtering a predeposited 30 nm thick metal layer. The polymer prepattern was removed by O_2 RIE (100 sccm, 20 mTorr) to obtain a high-aspect-ratio p–n heterostructure nanopattern with a scale width of 20 nm. To oxidize the p-n heterostructure nanopattern, the fabricated bimetal nanopattern was thermally annealed in a tubular furnace at 450°C for 3 hr to form a high-aspect-ratio WO_3/CuO nanopattern.
Characterization of the p–n heterojunction nanochannel: SEM (Magellan400, FE-SEM, FEI) was performed to obtain images of the materials. An electron beam incident energy between 1 and 10 kV was utilized. AFM (Park Systems, XE-100) was used to investigate closely the cross-sectional profiles of each patterned nanopattern. Crystallographic information was obtained on an X-ray diffractometer (Rigaku, D/MAX-2500). TEM (Tecnai G2 F30 S-Twin) was performed to obtain

high-resolution images of the pattern. To prepare the samples used in TEM, the patterned substrate from which the single p–n heterostructure nanopattern was detached was bladed on a Ni TEM grid. *Measurement systems of gas sensors:* To measure the resistance signal of the p–n heterostructure MOS nanopattern on the SiO_2/Si substrates, 75 nm thick Au electrodes having a predeposited 5 nm thick adhesion layer of Ti, as well as 100 μm spacing and width, were deposited by e-beam evaporation using a customized SERS mask.[29] The prepared p–n heterostructure MOS nanopattern sensors were mounted on a sensing chamber designed to measure resistance signals by using a data acquisition module (Agilent 34970A). The gas was passed through the sensing chamber. A gas delivery system designed in-house was used to control the gas flow into the sensing chamber to measure the sensor response to the analytes. The test analytes used in this study contained 1000 ppm of the VOCs toluene, acetone, ethanol, 100 ppm of ammonia, 10 ppm of nitric oxide for the selectivity test, and 10 ppm of ethanol for the dilution test. The serial dilution system used to control the gas concentration consisted of a mass flow controller (MFC, Brooks 5850E), Teflon tubing (PFA, 1/8"), Lok-type fitting, and valve system. Air was used as the reference gas, and the total flow rate for the reference gas and tested gas was maintained at 400 sccm.

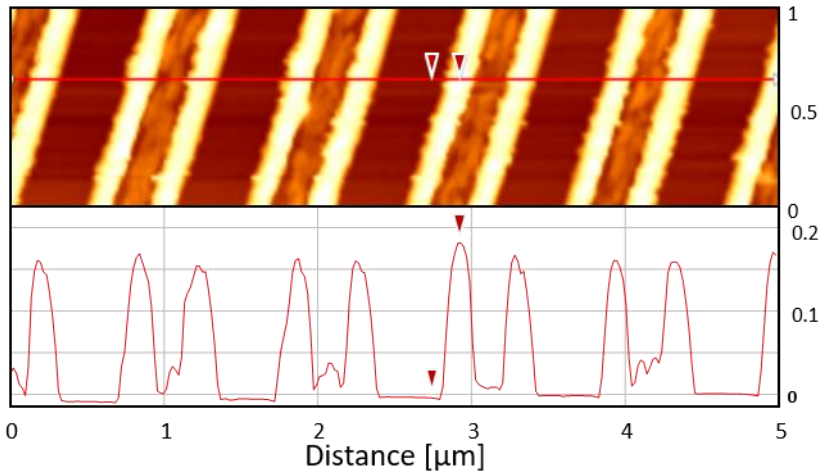

Figure S1. AFM profiles of the WO_3/CuO nanochannel.

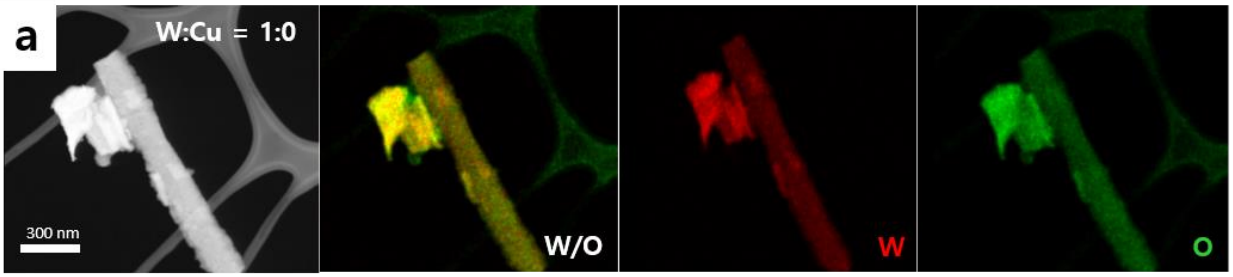

Figure S2. STEM EDS elemental mapping of WO_3 nanopattern without CuO heterojunction.

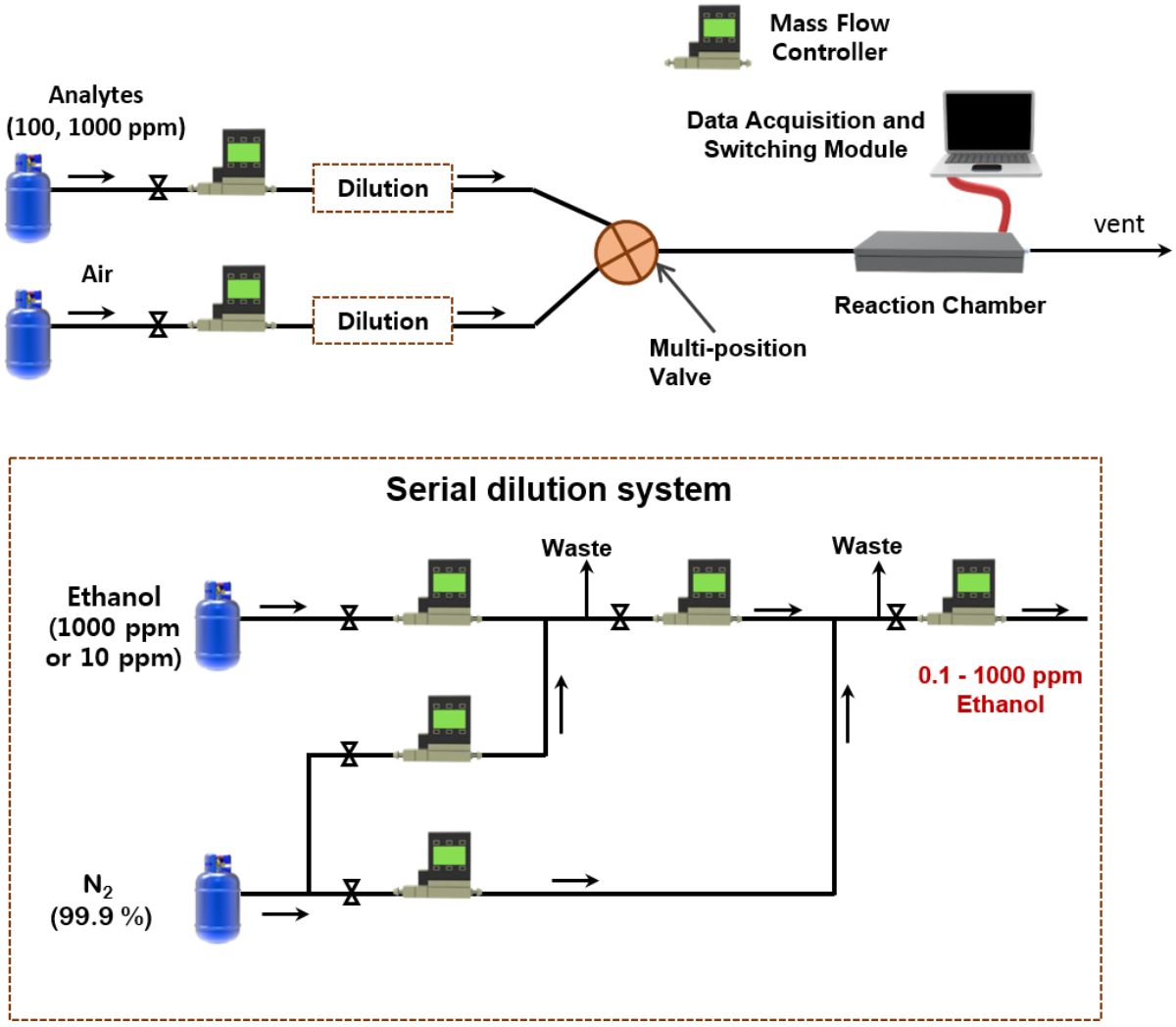

Figure S3. Schematic of the overall gas delivery system. Each analyte (toluene, hexane, acetone, and ethanol) and dry air was introduced in a controlled manner into the reaction chamber by using the MFC, tubing system, and multi-position valve. The serial dilution system was also used to obtain 0.1–1000 ppm concentrations of the analyzed gas.

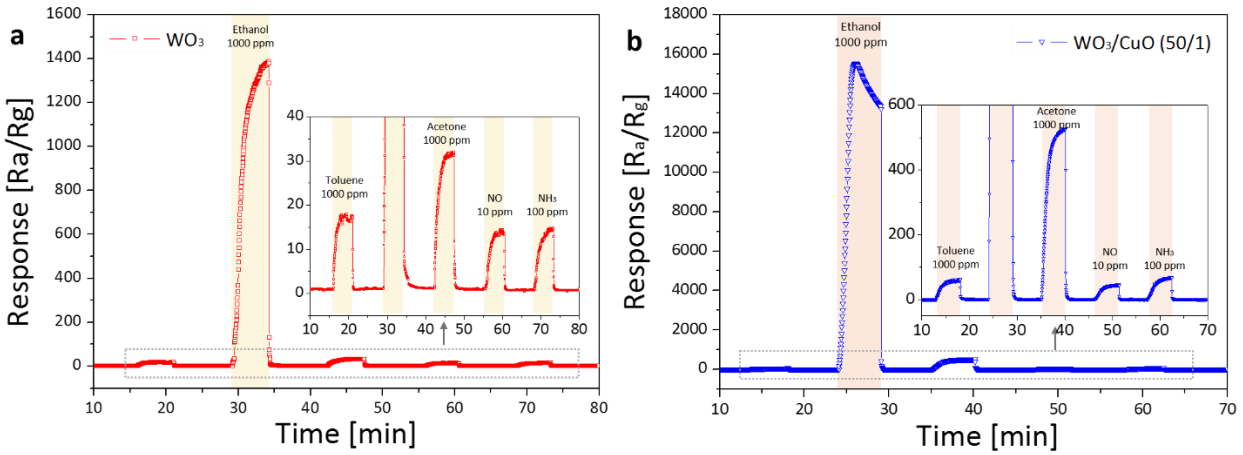

Figure S4. Real-time gas response of the (a) WO_3 and (b) WO_3/CuO (50/1) nanopattern sensors for various analytes (1000 ppm toluene, acetone, ethanol, 10 ppm NO, and 100 ppm NH_3). Both nanopatterns exhibited highly selective property toward 1000 ppm ethanol with high sensitivity.

Refs	Composite	Response (R_{air}/R_{gas})	Concentration (ppm)	Selectivity ($S_{ethanol}/S_{other\ gas}$)	Response / Recovery (s)	Operating T (℃)	Note
1	Nanoporous In2O3 hollow spheres	137.2	100 ppm	9 (H_2), 11 (CO), 39.2 (C_3H_8)	2 / 830	400	-
2	Ag nanoparticle -SnO_2 nanowire	228.1	100 ppm	30 (NH_3), 42 (H_2), 45 (CO)	0.8 / 80	450	-
3	Pt-doped In_2O_3 hollow spheres	4748 (1.2)	100 ppm (0.06 ppm)	267.9 (H_2), 390 (CO), 273.4 (C_3H_8)	0.4-1.27 / 239	371	Narrow detection range (2 ppm~ 100 ppm)
4	Hierarchical Au-loaded In2O3 hollow sphere	185.2	100 ppm	4.6 (CH_2O), 6.1 (C_3H_6O), 18.5(NH_3) 18 (C_6H_6), 19 (C_7H_8)	9 / 6	320	-
5	Ag-(TiO_2/SnO_2) porous nanostructures	53	50 ppm	4 (C_3H_6O), 5.3 (CH_3OH)	3.5 / 7	275	-
6	In/SnO2 nanoparticle	110	1000 ppm	All less than 100 (NO_2, H_2S, H_2, CH_4)	2 / -	300	-
7	Mesoporous In2O3 Particle	63.4	100 ppm	2 (CH_2O), 2.2 (C_3H_6O), 2.4 (CH_3OH)	2 / 45	220	-
8	SnO_2/ZnO nanofiber	78	100 ppm	7 (DMF), 4 (CH_3COOH), 3.5 (CH_3OH), 2.2 (CH_3COCH_3)	25 / 9	300	-
9	ZnO/TiO_2 nanorod	50.6	500 ppm	All less than 10 (H_2S, CH_4, C_3H_6O, CO, CH_3OH, C_2H_2)	5 / 10	320	-
10	Ni/SnO_2 hollow spheres	59	100 ppm	Not tried	2 / 15	280	-
11	SnO_2 Thin film	280	100 ppm	Not tried	55 / 17	300	-
12	Screen-printed SnO_2 nanowire	10.8	100 ppm	1.1 (C_3H_6O), 4.1 (CO), 3.5 (H_2)	4 / 30	400	-
13	SnO_2 nanoplate	1.59	1.5 ppm	Not tried	-	350	-
14	Pt-doped SnO_2 nanowire	8421	500 ppm	Not tried	48 / 2	200	-
15	Sb-doped SnO_2 nanowire	1.76	10 ppm	Not tried	1 / 5	300	-
16	SiO_2-doped SnO_2 film	318	50 ppm	Not tried	-	320	-
17	La_2O_3-doped SnO_2 nanowire	22.7	10 ppm	3.8 (C_3H_6), 3.5 (CO), 2.8 (H_2)	1 / 88	400	-
18	$ZnSnO_2$ nanowire	2.7	1 ppm	Not tried	1 / 1	300	-
19	$ZnSnO_4$ nanofiber	300	100 ppm	Up to 30 (CO, H_2)	-	450	-
20	Mn_3O_4-ZnO nanobelts	> 1.2	0.15 ppm (LOD)	4.69 (NH_3), 11.31 (CO), 18.14 (C_3H_8) 21.14 (H_2)	-	400	
This work	WO_3 patterned nanowire	1320	1000 ppm	77 (C_7H_8), 41 (C_3H_6O), 101 (NH_3), 94 (NO)	4 / 210	360	Wide detection range (0.1 ppm ~ 0.1 %)
This work	CuO/WO_3 patterned nanowire	15554 (75)	1000 ppm (0.094 ppb)	250 (C_7H_8), 30 (C_3H_6O), 338 (NH_3), 222 (NO)	2 / 120	360	

Figure S5. Comparison table of ethanol-sensing performance based on MOS. The blue-marked one is the best previous work so far; our work has much wider detection range, from part-per-billion level (100 ppb) to percent level (0.1%), with incomparable detection limit (R_a/R_g = 75 at 0.094 ppb), similar response time, and faster recovery property even at percent level concentration (120 sec at 0.1%).

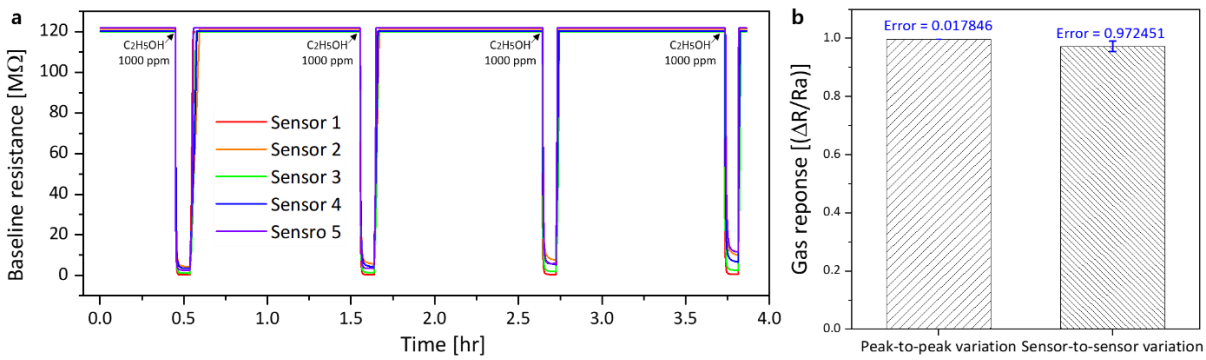

Figure S6. Reproducibility of the WO_3/CuO nanopattern sensors. (a) Real-time sensing responses of five WO_3/CuO nanopattern sensors with repetitive ethanol exposures. (b) Peak-to-peak reproducibility of single WO_3/CuO sensor and sensor-to-sensor reproducibility calculated from real-time data.

References

(1) Kim, S.-J. Hwang, I.-S. Choi, J.-K. Kang, Y. C. Lee, J.-H. *Sens. Actuator B* **2011**, *155, 512*

(2) Hwang, I.-S. Choi, J.-K. Woo, H.-S. Kim, S.-J. Jung, S.-Y. Seong, T.-Y. Kim, I. -D. Lee, J.-H. *ACS Appl. Mater. Interfaces* **2011**, *3, 3140*

(3) Kim, S.-J. Hwang, I.-S. Na, C.W. Kim, I. -D. Lee, Kang, Y. C. Lee, J.-H. *J. Mater. Chem*., **2011**, *21, 18560*

(4) Su Zhang, Peng Song, Huihui Yan, Qi Wang *Sens. Actuator B* **2016**, *231*, 245

(5) Vijay K. Tomer, Surender Duhan *J. Mater. Chem.*, **2016**, *4, 1033*

(6) K.Inyawilert, A.Wisitsoraat, C.Sriprachaubwong, A.Tuantranont, S.Phanichphant, C.Liewhiran *Sens. Actuator B* **2015**, *209, 40*

(7) Xiaohong Sun, Haoran Hao, Huiming Ji, Xiaolei Li, Shu Cai, and Chunming Zheng *ACS Appl. Mater. Interfaces* **2014**, *6, 401*

(8) S.H. Yan, S.Y. Ma, W.Q. Li, X.L. Xu, L. Cheng, H.S. Song, X.Y. Liang *Sens. Actuator B* **2015**, *221, 88*

(9) Jianan Deng, Bo Yu, Zheng Lou, Lili Wang, Rui Wang, Tong Zhang *Sens. Actuator B* **2013**, *184, 21*

(10) Yuejiao Chen, Ling Yu, Dandan Feng, Ming Zhuo, Ming Zhang, Endi Zhang, Zhi Xu, Qiuhong Li, Taihong Wang *Sens. Actuator B* **2012**, *166, 61*

(11) Liu, Y. Koep, E. Liu, M. *Chem. Mater*. **2005**, *17, 3997*

(12) Van Hieu, N. *Sens. Actuators, B* **2010**, *144, 425*

(13) Li, K.-M.; Li, Y.-J.; Lu, M.-Y.; Kuo, C.-I.; Chen, L.-J. *Adv. Funct. Mater.* **2009**, *19, 2453*

(14) Lin, Y.-H. Hsueh, Y.-C. Lee, P.-S. Wang, C.-C. Wu, J. M. Perng, T.-P. Shih, H. C. *J. Mater. Chem*. **2011**, *21, 10552*

(15) Wan, Q. Wang, T. H. *Chem. Commun.* **2005**, *41, 3841*

(16) Tricoli, A. Graf, M. Pratsinis, S. E. *Adv. Funct. Mater.* **2008**, *18, 1969*

(17) Nguyen Van Hieu, Kim, H.-R. Ju, B.-K. Lee, J.-H. *Sens. Actuators B: Chem*. **2008**, *133, 228*

(18) Xue, X. Y. Chen, Y. J. Wang, Y. G. Wang, T. H. *Appl. Phys. Lett*. **2005**, *86, 233101*

(19) Choi, S. H. Hwang, I. S. Lee, J. H. Oh, S. G.; Kim, I. D. *Chem. Commun.* **2011**, *47, 9315*

(20) Na, C. W. Park, S. Y. Chung, J. H. Lee, J. H. *ACS Appl. Mater. Interfaces* **2012**, *4, 6565.*